

This article was downloaded by:

On: 21 January 2011

Access details: *Access Details: Free Access*

Publisher *Taylor & Francis*

Informa Ltd Registered in England and Wales Registered Number: 1072954 Registered office: Mortimer House, 37-41 Mortimer Street, London W1T 3JH, UK



## International Reviews in Physical Chemistry

Publication details, including instructions for authors and subscription information:

<http://www.informaworld.com/smpp/title~content=t713724383>

### Spectroscopy and structure of solvated alkali-metal ions

James M. Lisy

Online publication date: 26 November 2010

**To cite this Article** Lisy, James M.(1997) 'Spectroscopy and structure of solvated alkali-metal ions', International Reviews in Physical Chemistry, 16: 3, 267 – 289

**To link to this Article:** DOI: 10.1080/014423597230208

**URL:** <http://dx.doi.org/10.1080/014423597230208>

PLEASE SCROLL DOWN FOR ARTICLE

Full terms and conditions of use: <http://www.informaworld.com/terms-and-conditions-of-access.pdf>

This article may be used for research, teaching and private study purposes. Any substantial or systematic reproduction, re-distribution, re-selling, loan or sub-licensing, systematic supply or distribution in any form to anyone is expressly forbidden.

The publisher does not give any warranty express or implied or make any representation that the contents will be complete or accurate or up to date. The accuracy of any instructions, formulae and drug doses should be independently verified with primary sources. The publisher shall not be liable for any loss, actions, claims, proceedings, demand or costs or damages whatsoever or howsoever caused arising directly or indirectly in connection with or arising out of the use of this material.

## Spectroscopy and structure of solvated alkali-metal ions

by JAMES M. LISY

Department of Chemistry, University of Illinois at Urbana-Champaign, Urbana,  
Illinois 61801, USA

Vibrational pre-dissociation spectroscopy combined with mass spectrometry has been used to obtain the infrared spectra of mass-selected cluster ions. The onset of new spectroscopic features, as a function of solvent number, has been shown to correspond to specific structural changes such as the filling of solvent shells and the formation of hydrogen bonds. These small finite systems offer a number of advantages over traditional solution-based measurements and perhaps are the most useful way to test current theoretical calculations and models. Whereas thermodynamic properties, derived from high-pressure mass spectrometry measurements, give some indication of solvent shell size, vibrational spectra suggest a more complex picture. When combined with recent infrared studies of size-selected neutral clusters, considerable detail of the solvent structure about the ion can be obtained. The solvation of the alkali-metal ions  $\text{Na}^+$  and  $\text{Cs}^+$  by a number of solvents, including water, will be discussed. Future directions and applications will be presented.

### 1. Introduction

The nature of ions in solution is a fundamental aspect of chemistry and biochemistry. While in the past, studies have primarily focused on the condensed phase, more recent efforts on the gas phase have endeavoured to examine solvation at the molecular or atomic level. The first experiments in this area used high-pressure mass spectroscopy (HPMS) to determine thermodynamic properties of ion solvation: the enthalpy and entropy of solvent association as a function of the number of solvents. These measurements offered a direct comparison with the bulk values from solution thermodynamics. The efforts of many researchers can be found in the literature [1]. It is interesting to note that collision-induced dissociation measurements are now being used to obtain association enthalpies with comparable accuracy [2] and offer a wider range of applications [3] (such as multiply charged species) than HPMS. A sharp change in the enthalpy of association with increasing solvent number has been used to signal the filling of a solvent shell. While these abrupt variations have been observed with the small alkali cations  $\text{Li}^+$  and  $\text{Na}^+$  and molecular ions  $\text{H}_3\text{O}^+$  and  $\text{NH}_4^+$ , smooth variations are observed for larger alkali cations and halide anions with no discernible indication of shell filling [1].

Spectroscopic studies of cluster ions offered the potential for a more detailed characterization of the fundamental interactions between ion and solvent. As a result, there have been a number of efforts covering the electromagnetic spectrum from the infrared to the ultraviolet with a wide range of cluster types, such as solvated electrons, protonated ions and solvated metal ions. In addition, the intrinsic charge on these ions permits size- and composition-selective studies to be routinely accomplished using mass spectrometry methods. This was an important advantage over neutral cluster studies, although recent efforts by Huisken *et al.* on neutral clusters of HF [4],  $\text{H}_2\text{O}$  [5] and  $\text{CH}_3\text{OH}$  [6] have established a major breakthrough in this area. In a somewhat interesting twist, these recent results for neutral clusters have greatly assisted the

interpretation of infrared spectra of solvated ions as will be discussed later in this paper.

The effects of solvation on the properties of an ion have been examined by many groups. Negative-ion clusters have been studied via photodissociation and photo-detachment, for example, in [7–10] using visible or ultraviolet laser excitation. As in the case of HPMS thermodynamics results, abrupt changes in the photofragment distribution or the photoelectron spectrum as a function of solvent number were used to infer solvent shell effects. Similar studies using electronic pre-dissociation, by Farrar and co-workers on  $\text{Sr}^+$  solvated by water [11] and ammonia [12] and by Fuke and co-workers on the hydration of monovalent calcium [13] and magnesium [14] ions, have examined the possible role of charge transfer in the size-dependent variation of the electronic spectra. In addition, there have been a number of investigations on binary complexes containing either a monovalent alkaline-earth or transition-metal ion by Duncan and co-workers [15] and Brucat and co-workers [16] respectively, producing valuable details on the nature of metal–ligand binding.

Infrared studies have perhaps been the most versatile method in the study of ion–molecule interactions, as different vibrational modes display different behaviours when complexed to an ion. In the 9–10  $\mu\text{m}$  region, the  $\nu_2$  umbrella mode in ammonia shifts to a higher frequency when complexed to an ion such as  $\text{Na}^+$  or  $\text{NH}_4^+$ , as has been shown by Selegue and Lisy [17] and Kondow and co-workers [18] respectively. Conversely, the C—O stretch in methanol shifts to lower frequency when complexed to the sodium [19] or a caesium [20] cation. Other studies in this region have examined the effects of solvation on the central ion as demonstrated by Stace and co-workers for  $\text{SF}_6^+$  solvated by argon [21],  $\text{C}_6\text{H}_6$  [22],  $\text{CO}_2$  [23] and  $\text{NO}$  [24].

Perhaps the most interesting infrared work has been done in the 3  $\mu\text{m}$  region. Detailed structural information on ion–molecule interactions in binary complexes have been obtained by Maier and co-workers on a number of ions such as  $\text{N}_2\text{H}^+$ ,  $\text{HCO}^+$  and  $\text{NH}_4^+$  complexed with a rare gas [25] and for  $\text{HCO}^+ - \text{H}_2$  [26]. The hydration of halide anions can be ideally studied in this region as shown by Okumura and co-workers for chloride [27] and iodide [28], where the competition between electrostatic and hydrogen bonding plays a particularly crucial role. Okumura and co-workers have also observed significant changes in both the infrared spectra and the photodissociation dynamics of  $\text{NO}^+(\text{H}_2\text{O})_n$  [29] and  $\text{NO}_2^+(\text{H}_2\text{O})_n$  [30]. In most ion cluster studies either the properties of the ion or the solvent are probed. With molecular ions, both perspectives can be viewed simultaneously. This latter situation is best described by the pioneering work of Lee and co-workers on  $\text{H}_3^+(\text{H}_2)_n$  [31],  $\text{H}_3\text{O}^+(\text{H}_2)_n$  [32],  $\text{NH}_4^+(\text{NH}_3)_n$  [33],  $\text{CH}_5^+(\text{H}_2)_n$  [34], and by Mikami and co-workers on cluster ions of phenol with water [35, 36] and methanol [36].

In this review, we shall focus on the solvation of metal ions, specifically alkali-metal ions for a number of reasons. First and foremost, the closed shell of the alkali ions will restrain the reactants to the ground electronic state and greatly reduce the possibilities that chemistry will occur. Thus the primary interaction between the ion and the solvent is electrostatic. This is commonly viewed in the process of solvation as the principal effect in disrupting or enhancing the structure of the solvent. However, it should be noted that dehydration of methanol to dimethyl ether has been observed for all methanol-solvated alkali metal ions, and that the chemistry appears to be size selective [37]. Second, in keeping with the rather simple nature of the system, the intrinsic interplay between the ion–solvent and solvent–solvent interactions can be examined. This information not only serves as a check to *ab initio* calculations on

solvated ion structures [38], but as a test for the many intermolecular model potentials used in molecular simulations [39], by supplying size- and composition-specific experimental results for comparison. If the model potentials fail to reproduce the experimental observations, one could justifiably question any quantitative conclusions based on those potentials when applied to other systems. Third, these studies will enable us to evaluate the popular model of solvation with well established concentric shells, without substantial complications from chemical interactions.

## 2. Experimental approaches

In the spectroscopic study of gas-phase ion solvation, there are three obvious requirements: the generation of cluster ions, a method for mass selection and a choice of spectroscopic probes. The mass spectrometry methods are naturally partitioned into two categories: time-of-flight (TOF) methods and mass filters. The latter method includes Wien filters, ion traps, quadrupoles and magnetic–electric sector instrumentation. Essentially all the TOF methods use reflectrons and/or mass gates for achieving MS–MS capability. Both general methods have been successfully applied to the infrared spectroscopy of cluster ions: Okumura [27–30] using the TOF method, while Kondow [18], Lee [31–34], Lisy [17, 19, 20], Maier [25, 26], Mikami [35, 36] and Stace [21–24] have used mass filters of one type or another. The choice of the mass spectrometry method is not necessarily driven by the type of ion cluster source. As Maier [25, 26], Mikami [35, 36] and Stace [21–24] have shown, a pulsed source can be readily used with mass filters, in contrast with the more typical combination of continuous ion sources with mass filters. Okumura [27–30] has made the more natural selection of teaming his pulsed nozzle source with a TOF mass spectrometer.

There has also been a significant variety in the types and approaches to cluster ion sources by the various groups. Starting first with the pulsed methods, Okumura [27–30] generated cluster ions either by crossing an electron beam near the exit of a pulsed nozzle or by inducing an electrical discharge in a channel downstream from the nozzle. Electron guns were also used by Maier [25, 26] and Stace [21–24], the latter using ‘pick-up’ techniques to attach the molecule of interest to a cluster of solvent molecules prior to ionization. Mikami [35, 36] combined a pulsed ultraviolet laser, to produce an aromatic ion core via resonance enhanced multiphoton ionization (REMPI), with a pulsed nozzle to generate cluster ions. The variety of continuous nozzle methods are equally wide ranging. Kondow [18] used the most traditional approach with an electron gun to generate cluster ions from a skimmed conventional aperture nozzle source. Lee [31–34] has adapted, with great success, a high-pressure corona discharge source [40] to produce cold cluster ions. Lisy [17, 19, 20] has used a different approach of generating cluster ions by injecting cations from thermionic emitters into fully expanded continuous jets.

All the infrared spectroscopy to date has been confined to two spectral regions: 9–10  $\mu\text{m}$ , accessible using  $\text{CO}_2$  lasers, and 2.5–4  $\mu\text{m}$ , using difference frequency generation and optical parametric oscillators (OPOs) with  $\text{LiNbO}_3$  as the active gain medium. Straightforward single-photon vibrational pre-dissociation spectroscopy has been used by Kondow [18], Lisy [17, 19, 20] and Stace [21–24] with line-tunable  $\text{CO}_2$  lasers of either commercial or home-made manufacture. The systems studied have either exhibited sufficiently weak binding or possessed ample internal energy so that the absorption of a single photon with about 10–11  $\text{kJ mol}^{-1}$  would induce dissociation. Similar experiments in the 2.5–4  $\mu\text{m}$  region with corresponding photon energies of about 30–50  $\text{kJ mol}^{-1}$  have been performed by Okumura [27–30], Lee

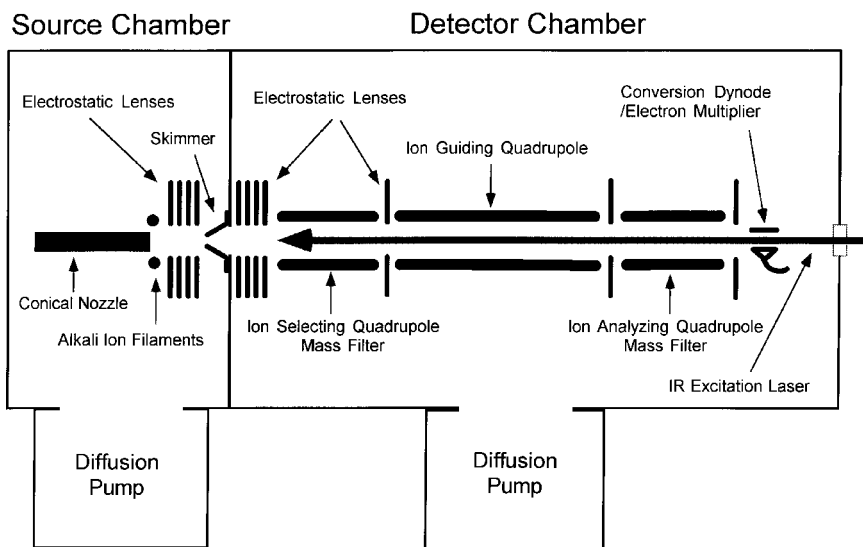


Figure 1. Triple quadrupole mass spectrometer apparatus for the generation, photodissociation and detection of solvated metal ion clusters.

[31–34], Maier [25, 26], and Mikami [35, 36] and recently Weinheimer and Lisy [41, 42, 43] on a variety of hydrogen-bonded systems. In general, these latter photodissociation experiments have required only a single photon. However, for some of the smallest cluster ions with the highest binding energies, this has not been sufficient. Multiphoton absorption of the tunable infrared radiation was thought to lead to dissociation for  $\text{NH}_4^+(\text{NH}_3)_{3-10}$  [33],  $\text{Cl}^-(\text{H}_2\text{O})$  [27] and  $\text{phenol}^-(\text{H}_2\text{O})_{1-4}$  [35, 36]. For the most tightly bound systems  $\text{NH}_4^+(\text{NH}_3)_{1,2}$  [33] and  $\text{H}^+(\text{H}_2\text{O})_{2-4}$  [32], a  $\text{CO}_2$  laser was used for multiphoton dissociation following the absorption of a single tunable infrared laser photon from either a difference frequency or a colour centre laser respectively.

While the experimental details may vary among the various groups, the operational procedures are the same for all these studies. Following the production of the cluster ions, a specific species is mass selected for investigation. Using the triple quadrupole method from our laboratory [41–43] as an example, this is accomplished with the first quadrupole mass filter in the apparatus shown in figure 1. With the cluster of interest now isolated, it is allowed to interact with one (or more) infrared laser(s). In the triple quadrupole, this is done by passing the laser along the axis of all three quadrupoles. In the case of the pulsed  $\text{LiNbO}_3$  OPO [41–43], time discrimination is used to isolate the interaction between the OPO and the ion clusters to the region of the middle quadrupole. This middle quadrupole operates in a rf-only mode and acts as an ion guide for the initial cluster ion and any product ions resulting from the interaction with the laser. Vibrational pre-dissociation is detected by monitoring the composition of the ion clusters from the second quadrupole with the third mass-analysing quadrupole. If tuned to the same mass as the first quadrupole, any decrease in the ion cluster beam intensity would be indicative of absorption of a photon leading to dissociation. A more sensitive mode of operation has the quadrupole tuned to a mass corresponding to the loss of one solvent molecule, the most typical photodissociation outcome. The ion beam intensity at this mass value with the laser 'off' will be quite low and the detection of vibrational pre-dissociation can be performed with a better signal-to-noise ratio as shown in figure 2. This procedure is repeated at different laser

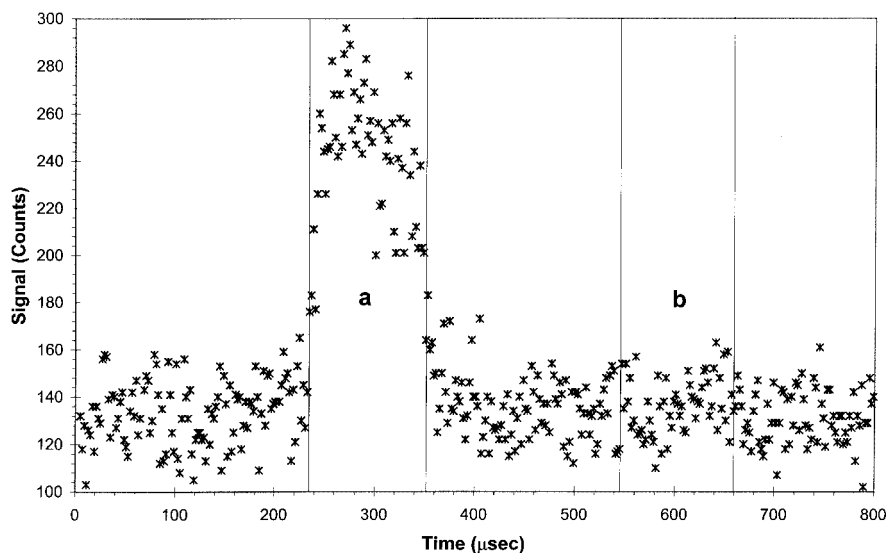


Figure 2. Output of the multichannel scalar of the photodissociation of  $\text{Cs}^+(\text{CH}_3\text{OH})_3$  detecting the  $\text{Cs}^+(\text{CH}_3\text{OH})_2$  fragment ion. The channels in region a correspond to the interaction between the OPO and the mass-selected  $\text{Cs}^+(\text{CH}_3\text{OH})_3$  in the middle quadrupole. The signal, resulting from subtraction of the background in region b due to CID and spontaneous dissociation from region a, is proportional to the photodissociation cross-section, when corrected for the laser fluence.

frequencies. If one assumes that the absorption of a photon leads to dissociation, the fraction of cluster beam that loses a solvent molecule can be related to the photoabsorption cross-section, when corrections for the variation in laser intensity or fluence are taken.

### 3. Vibrational spectra

Until recently, vibrational spectra on solvated metal ions had been confined to the 9–10  $\mu\text{m}$  region of the infrared. This limited the types of solvent molecules available for study. Furthermore, since the goal was to observe size-dependent behaviour in the solvation process, the vibrational modes in this spectral region needed to be sensitive to either interaction with the ion or to other solvent molecules. In spite of these obvious restrictions, two molecules  $\text{CH}_3\text{OH}$  and  $\text{NH}_3$  proved to be more than adequate. The C—O stretch had been shown to be a sensitive probe of hydrogen bonding in earlier research on neutral methanol clusters [44]. Similarly, the  $\nu_2$  umbrella mode of ammonia had also been observed to be susceptible to intermolecular interactions in neutral clusters [45] and in matrix isolation studies [46] when complexed to  $\text{Na}^+$ . It was also hoped that the C—N stretch in methylamine would have similar sensitivity, based on neutral cluster studies [47]. However, the only variation in the vibrational pre-dissociation spectra of  $\text{Cs}^+(\text{CH}_3\text{NH}_2)_{3-22}$  was a slight shift of  $5\text{ cm}^{-1}$  in a single band with 14–15 solvents, suggesting some sort of rearrangement [48].

The vibrational pre-dissociation spectra of  $\text{Cs}^+(\text{CH}_3\text{OH})_{4-25}$  [20] and  $\text{Na}^+(\text{CH}_3\text{OH})_{3-25}$  [19] in the 1020–60  $\text{cm}^{-1}$  region were obtained using a single quadrupole apparatus. The onset of new vibrational bands in the spectra were assigned to the occupation of new structural environments, or solvent shells. In the case of  $\text{Cs}^+(\text{CH}_3\text{OH})_n$ , the first solvent shell was observed to fill at  $n = 10$ , with the onset of a new band for  $n = 11$ . The next new band was first observed at  $n = 18$  while,

at a size too small to be consistent with the filling of the second solvent shell, this was interpreted as the binding of small clusters of methanol to the surface of the solvated ion, or what could be described as a 'bulk' solvent. Similar observations were observed in the case of  $\text{Na}^+(\text{CH}_3\text{OH})_n$ , but at different values of  $n$ . This reflected the difference in the electrostatic interaction due to the smaller ionic radius (or alternatively the higher charge density) of the  $\text{Na}^+$ . The first solvent shell for  $\text{Na}^+(\text{CH}_3\text{OH})_n$  was observed to fill at  $n = 6$ . Subsidiary structural changes were observed at  $n = 15$  and  $22$ . The former was suggestive of the filling of a second solvent shell, with the latter correlating to the onset of a 'bulk-like' environment. The differences between the two systems were what one would generally expect; the smaller  $\text{Na}^+$  ion was more disruptive of the liquid methanol structure. This was supported by the observations of a smaller first solvent shell, more numerous solvent environments and a larger number of solvents needed to reach the 'bulk' solvent limit. Substantial Monte Carlo simulations [19, 20] were performed in conjunction and support of the experimental studies. The size of the solvent shells and the onset of new solvent environments were found to be consistent with the experimental observations. There were also predictions made concerning the onset of hydrogen-bond formation for both systems. For  $\text{Cs}^+(\text{CH}_3\text{OH})_n$ , hydrogen bonding was predicted [20] to occur first around  $n = 8$ , in a manner that was expected to stabilize the formation of the first solvent shell at  $n = 10$ . With  $\text{Na}^+(\text{CH}_3\text{OH})_n$ , no hydrogen bonding was expected until the occupation of the second solvent shell commenced at  $n = 7$ . Studies of these clusters in the  $3000\text{--}3800\text{ cm}^{-1}$  region were proposed to test the validity of the predictions. These will be discussed below.

Vibrational pre-dissociation spectra of  $\text{Na}^+(\text{NH}_3)_{6-12}$ , in the  $1020\text{--}1090\text{ cm}^{-1}$  region [17] were obtained to examine the ion–ammonia and ammonia–ammonia interactions on the  $\nu_2$  umbrella mode of ammonia. The sensitivity of this mode is quite remarkable. Shifts of over  $100\text{ cm}^{-1}$  to higher frequency and in excess of 10% of the unperturbed fundamental have been observed in neutral clusters [45] and other complexes [46]. Indeed, strong electrostatic interactions with the  $\text{Na}^+$  ion, shifted the vibrational frequency of this mode beyond the tuning range (greater than  $1090\text{ cm}^{-1}$ ) of the  $\text{CO}_2$  laser for  $\text{Na}^+(\text{NH}_3)_{n \leq 6}$ . The vibrations then shifted to lower frequency when molecules began to occupy the second solvent shell for  $n \geq 7$ . The somewhat weaker hydrogen-bonding capability of ammonia together with a larger polarizability, when compared with methanol, led to the onset of a bulk-like environment for ammoniated sodium ions with about ten solvent molecules. This was substantially less than was observed for  $\text{Na}^+(\text{CH}_3\text{OH})_n$ .

These early studies of metal ion solvation were instrumental in understanding the most fundamental aspects of the solvation process in the gas phase: the size of the first solvent shell, the number of solvent environments and the onset of bulk-like solvent behaviour. However, they did not address the more important questions having to do with the competition between ion–neutral and neutral–neutral interactions. The most important facet of this question entails the interplay between hydrogen bonding and the electrostatic interaction involving the ion and a solvent such as water or methanol. Not only are these issues important to the understanding of solvation at the microscopic level, but also they are of fundamental interest in the area of ion transport in biological systems [49].

There has been substantial progress in addressing the basic nature of solvation with recent experiments in the  $3\text{ }\mu\text{m}$  region. As mentioned earlier, Lee and co-workers have addressed the role of hydrogen bonding in a variety of protonated complexes of

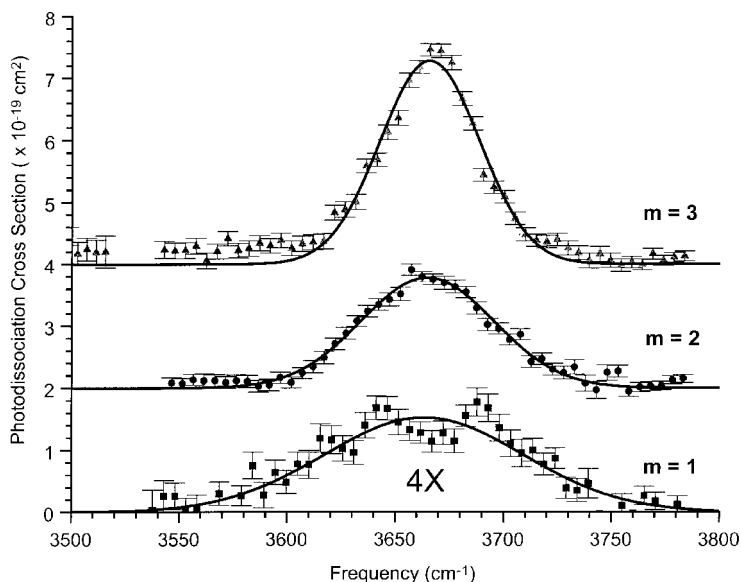


Figure 3. Vibrational photodissociation spectra of  $\text{Cs}^+(\text{CH}_3\text{OH})_{1-3}$ . The error bars represent  $\pm 2\sigma$ . The curves are single Gaussian fits to the data.

hydrogen [31], water [32], ammonia [33] and methane [34]. However, molecular ions with their unique type of hydrogen-bonding interactions do not represent the simple electrostatic interactions of closed shell ions. The investigations by Okumura and co-workers [27, 28] on halide anion solvation by water show great promise but are still in the early stages. We have recently reported the vibrational pre-dissociation spectroscopy of  $\text{Cs}^+(\text{CH}_3\text{OH})_{1-6}$  [43],  $\text{Na}^+(\text{CH}_3\text{OH})_{2-7}$  [42] and  $\text{Cs}^+(\text{H}_2\text{O})_{1-5}$  [41] in the 3200–3800  $\text{cm}^{-1}$  region using a triple quadrupole mass spectrometer and a  $\text{LiNbO}_3$  OPO to excite the O—H stretch directly. As will be seen below, the rich spectra will not only let us address the role of hydrogen bonding in these cluster ions, but to reach some significant conclusions on the nature of ion solvation.

The solvated alkali metal ions are all generated by the collision between pre-formed neutral solvent clusters and a thermionic emitted ion. The collision energy in the centre of mass frame is typically a few electronvolts [50]. The nascent cluster ion has considerable internal energy which is dissipated primarily by evaporation. The amount of internal energy decreases as a function of time in a manner that has been modelled by the ‘evaporative ensemble’ developed by Klots [51]. The relevant time scale in our experiments is the flight time from the ion source to the entrance of the middle quadrupole, where mass-selected cluster ions are made available for infrared photodissociation. These times are approximately in the range 100–200  $\mu\text{s}$ . The amount of internal energy in the solvated ions varies with the size. Smaller cluster ions with higher binding energies have higher ‘temperatures’ than larger cluster ions. They can range from about 500 K for two solvents to about 280 K for six or more, depending on the solvent and ion. Clearly, cluster ions produced in this manner are ‘warm’ and very different from neutral clusters produced in molecular beam expansions with internal temperatures of a few kelvins.

The choice of methanol as the initial solvent was made to simplify the spectra as much as possible. Only the single O—H stretch is expected to absorb in the 3200–3800  $\text{cm}^{-1}$  range. As can be seen in figure 3, the vibrational spectra of



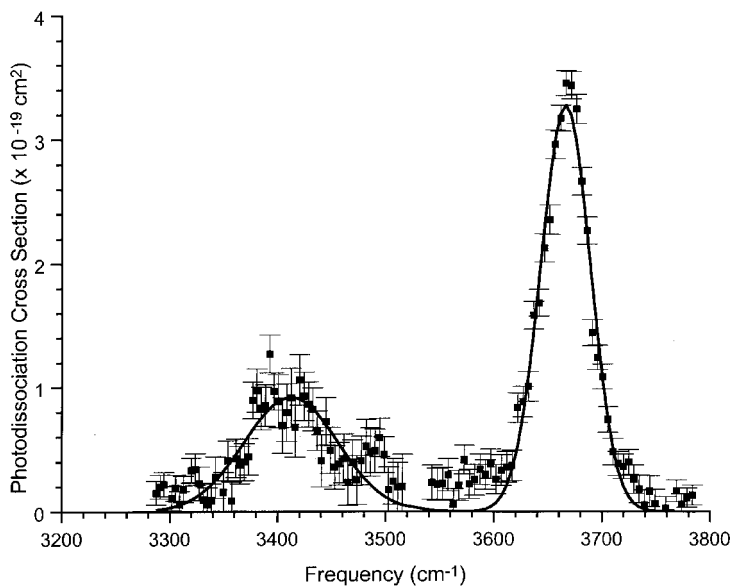


Figure 4. Vibrational photodissociation spectrum of  $\text{Cs}^+(\text{CH}_3\text{OH})_3$ . The error bars represent  $\pm 2\sigma$ . The curve is a double Gaussian fit to the data.

$\text{Cs}^+(\text{CH}_3\text{OH})_{1-3}$  in the region from 3500 to 3800  $\text{cm}^{-1}$  shows a single vibrational band shifted approximately 15  $\text{cm}^{-1}$  to a lower frequency than the value of the O—H stretch of gas-phase methanol [52] at 3681  $\text{cm}^{-1}$ . The linewidth decreases with increasing cluster size, which suggests that the temperature of the cluster also decreases, as would be expected within the evaporative ensemble model. There is no suggestion of hydrogen bonding in this spectral region. Scanning to lower frequencies for  $\text{Cs}^+(\text{CH}_3\text{OH})_{1,2}$  revealed no additional features. However, scanning to lower frequency for  $\text{Cs}^+(\text{CH}_3\text{OH})_3$  resulted in the spectrum shown in figure 4. As is apparent, the feature observed at 3414  $\text{cm}^{-1}$  is a clear indication of hydrogen bond formation. This early onset is in sharp contrast with the Monte Carlo simulations [20] that anticipated the onset of hydrogen-bond formation at  $\text{Cs}^+(\text{CH}_3\text{OH})_8$ . The structural moiety responsible for this feature will be discussed shortly. We can make the following observation at this time: the O—H vibrational frequency of methanols that only interact with the  $\text{Cs}^+$  are only slightly perturbed (10–15  $\text{cm}^{-1}$ ) from the gas-phase value. We shall use the term ‘isolated’ to characterize those molecules whose interactions are with the ion, and not with other solvent molecules about the ion. We also note that the band at 3415  $\text{cm}^{-1}$  for  $\text{Cs}^+(\text{CH}_3\text{OH})_3$  is rather weak in intensity for a hydrogen-bonded species. This suggests that the moiety responsible for this band may be only a minor contributor to the ion beam intensity at the  $\text{Cs}^+(\text{CH}_3\text{OH})_3$  mass peak and indicates the strong possibility of structural isomers in the beam. Finally, the shift to the lower frequency of 250  $\text{cm}^{-1}$  indicates that the value for the vibrational frequency of the methanol O—H stretch will be primarily determined by methanol–methanol interactions and not the ion–methanol interaction.

The spectra of the larger solvated ions  $\text{Cs}^+(\text{CH}_3\text{OH})_{4,5}$  display a steady increase in the extent of hydrogen bonding with increasing solvent number. In figure 5, the peak at about 3665  $\text{cm}^{-1}$  due to isolated methanol decreases in relative intensity at the expense of the hydrogen-bonded features in the 3300–3600  $\text{cm}^{-1}$  region. There are also more discernible peaks in the hydrogen-bonded region at about 3520, 3420 and

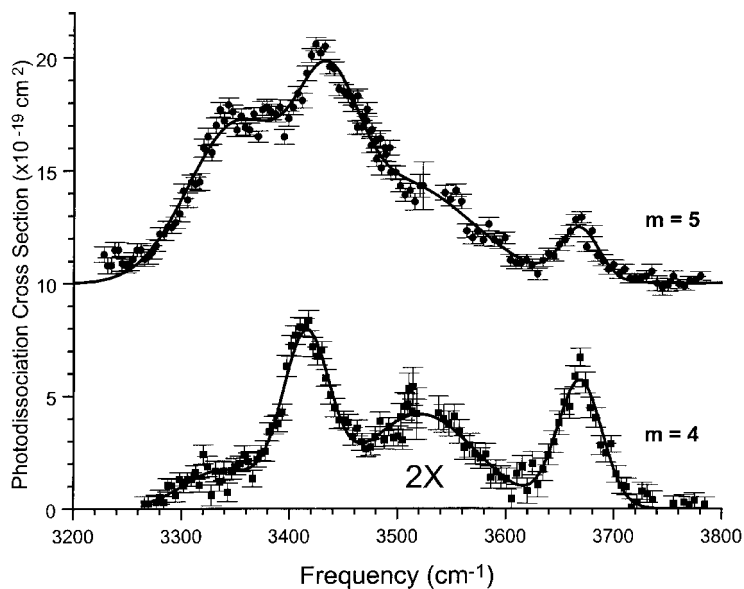


Figure 5. Vibrational photodissociation spectra of  $\text{Cs}^+(\text{CH}_3\text{OH})_{4,5}$ . The error bars represent  $\pm 2\sigma$ . The curves are multiple Gaussian fits to the data.

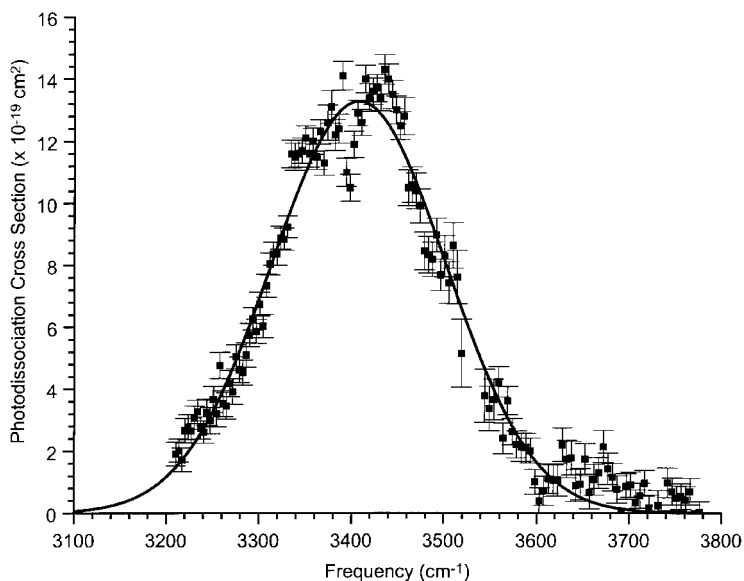


Figure 6. Vibrational photodissociation spectrum of  $\text{Cs}^+(\text{CH}_3\text{OH})_6$ . The error bars represent  $\pm 2\sigma$ . The curve is a single Gaussian fit to the data.

$3350\text{ cm}^{-1}$ . As we observed above, the values of the O—H vibrational frequencies are determined by the nature of the methanol—methanol interaction. These three separate peaks thus imply the existence of three different hydrogen-bonding environments coexisting with isolated methanols, all of which are located within the first solvent shell of  $\text{Cs}^+$ , a rather remarkable occurrence. The relative population in these different environments is also size-dependent. To close out this series of spectra, figure 6

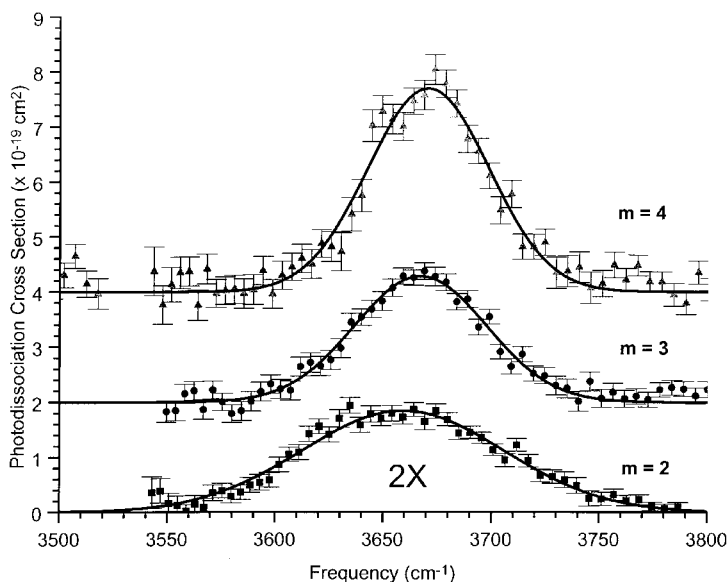


Figure 7. Vibrational photodissociation spectra of  $\text{Na}^+(\text{CH}_3\text{OH})_{2-4}$ . The error bars represent  $\pm 2\sigma$ . The curves are single Gaussian fits to the data.

contains the vibrational pre-dissociation spectrum of  $\text{Cs}^+(\text{CH}_3\text{OH})_6$ . At this point, it appears that hydrogen bonding has taken the upper hand in the competition with electrostatic interaction. There is essentially no intensity in the region associated with isolated methanols. The hydrogen-bonded region has also lost much of the structural richness associated with the small cluster ions. This is suggestive of an environment that is somewhat uniform, that is all the methanols are acting as proton donors and acceptors at this point and the  $\text{Cs}^+$  is incapable of disrupting the hydrogen-bonded network that exists in liquid methanol.

The number of hydrogen-bonded features in these spectra together with the relatively large linewidths indicate that the cluster ions possess significant internal energy. This in turn suggests that the structural isomers with energies near that of the global minimum may also be present in the mass-selected cluster ion beam and are responsible for the different hydrogen-bonded vibrational bands.

The replacement of  $\text{Cs}^+$  by  $\text{Na}^+$  allows us to examine directly the dependence of the cluster ion structure on the magnitude of the electrostatic interaction. Side-by-side comparisons for a given number of solvents will delineate these differences. As shown in figure 7, the first set of spectra for  $\text{Na}^+(\text{CH}_3\text{OH})_{2-4}$ , while similar to the smallest of the methanol-caesium ion clusters, have a number of differences. The onset of hydrogen bonding was observed for three methanols in the case of  $\text{Cs}^+$ , with rather substantial hydrogen bonding occurring for the next largest species as shown in figures 4 and 5.  $\text{Na}^+(\text{CH}_3\text{OH})_n$  displays no hydrogen bonding at  $n = 3$ , and just the slightest hint at  $n = 4$  (*vide infra*). Substantial hydrogen bonding is finally observed for  $\text{Na}^+(\text{CH}_3\text{OH})_{5-7}$ , as shown in figure 8. While the extent of hydrogen bonding increases with increasing cluster size, there is still substantial intensity in the  $3670\text{ cm}^{-1}$  region associated with isolated methanols through  $n = 7$ . Recall for  $\text{Cs}^+(\text{CH}_3\text{OH})_6$ , there was essentially no presence of isolated methanols, and there was little evidence for any distinct hydrogen-bonded environments as shown in figure 6. Contrasting this with the substantial structure observed in  $\text{Na}^+(\text{CH}_3\text{OH})_7$ , it is very clear that charge density

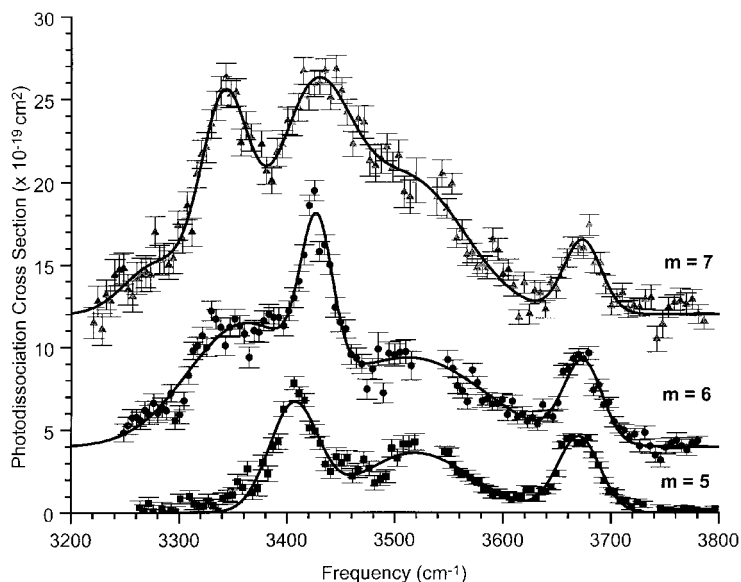


Figure 8. Vibrational photodissociation spectra of  $\text{Na}^+(\text{CH}_3\text{OH})_{5-7}$ . The error bars represent  $\pm 2\sigma$ . The curves are multiple Gaussian fits to the data.

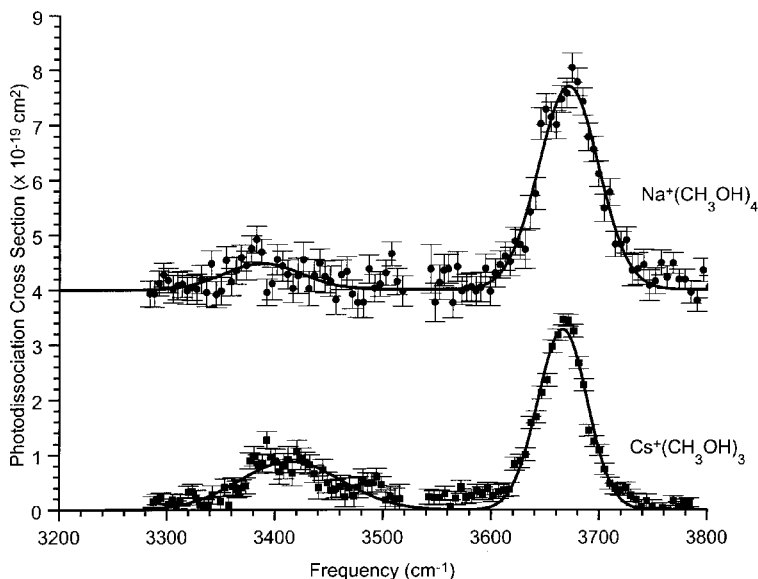


Figure 9. A comparison between the vibrational photodissociation spectra of  $\text{Cs}^+(\text{CH}_3\text{OH})_3$  and  $\text{Na}^+(\text{CH}_3\text{OH})_4$ . The error bars represent  $\pm 2\sigma$ . The curves are double Gaussian fits to the data. Note that the positions of the bands are very similar.

does play an important role in the structure of the cluster ion and that the balance between electrostatic and hydrogen-bond interactions is readily changed by going from  $\text{Cs}^+$  to  $\text{Na}^+$ . It is obvious that  $\text{Na}^+$  is much more capable of disrupting the hydrogen-bonded structure of methanol by first delaying the onset of hydrogen bonding and second by maintaining distinct solvent environments for a larger number

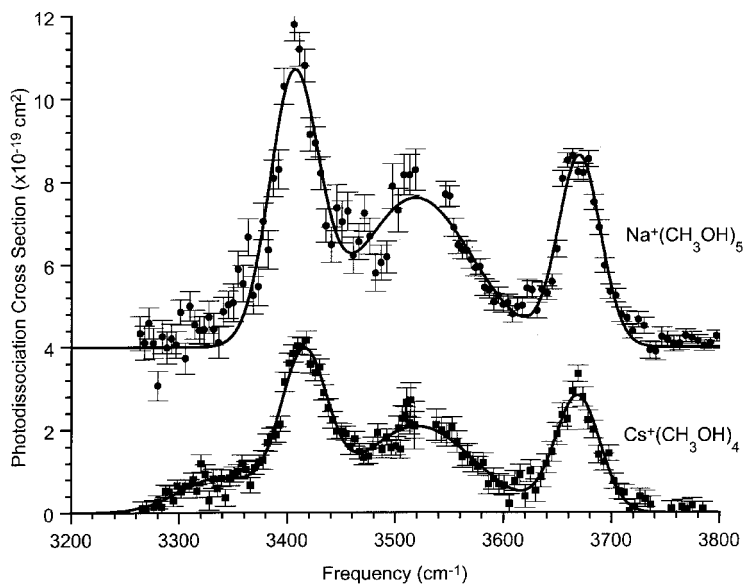


Figure 10. A comparison between the vibrational photodissociation spectra of  $\text{Cs}^+(\text{CH}_3\text{OH})_4$  and  $\text{Na}^+(\text{CH}_3\text{OH})_5$ . The error bars represent  $\pm 2\sigma$ . The curves are multiple Gaussian fits to the data. Note that the positions of the major bands are very similar.

of solvents. One final observation relates to the sensitivity of the O—H stretch to the filling of the solvent shell. In the  $\text{CO}_2$  laser vibrational pre-dissociation study of  $\text{Na}^+(\text{CH}_3\text{OH})_n$ ,  $n = 3\text{--}25$ , the first solvent shell was observed to fill [19] at  $n = 6$ . This was inferred from the onset of a new vibrational band of the C—O stretch at  $n = 7$ , shifted a few wavenumbers to higher frequency than the band observed for the smaller solvated ions. Similar behaviour was observed earlier for  $\text{Cs}^+(\text{CH}_3\text{OH})_n$ , but with the filling completed [20] at  $n = 10$ . There is no truly abrupt change in the O—H stretching spectra that could be attributed to the filling of the first solvent shell for the  $\text{Na}^+(\text{CH}_3\text{OH})_{5-7}$  cluster ions shown in figure 8. This further reinforces the observation that the vibrational frequencies for the methanol O—H stretch are determined by solvent–solvent and not ion–solvent interactions. It also suggests that different vibrational modes are sensitive to different environmental aspects with the methanol C—O stretch apparently more sensitive to the electrostatic presence of the ion.

While noting the contrasts in the vibrational spectra of  $\text{Na}^+(\text{CH}_3\text{OH})_n$  and  $\text{Cs}^+(\text{CH}_3\text{OH})_n$  above, the astute reader may have observed that there were simultaneously pronounced similarities but at different cluster sizes. We would now like to examine this more closely. The next three figures compare the vibrational spectra of  $\text{Cs}^+(\text{CH}_3\text{OH})_n$  with  $\text{Na}^+(\text{CH}_3\text{OH})_{n+1}$  for  $n = 3\text{--}5$ . In figure 9, the onset of hydrogen bonding in both systems is shown. Both cluster ions show the first of the hydrogen-bonded bands occurring at essentially the same frequency near  $3400\text{ cm}^{-1}$ . Figures 10 and 11 display the next two larger cluster ions in the series of both species. While there is some variation in the relative intensities of the vibrational bands, the vibrational frequencies are again essentially identical. Since the vibrational frequencies of the methanol O—H stretch are determined by the nature of the methanol–methanol interaction, these observations lead one to conclude that the hydrogen-bonding environments in both cluster ions are identical, while the relative population of a given environment is determined by the number of solvents and the size of the ion. The

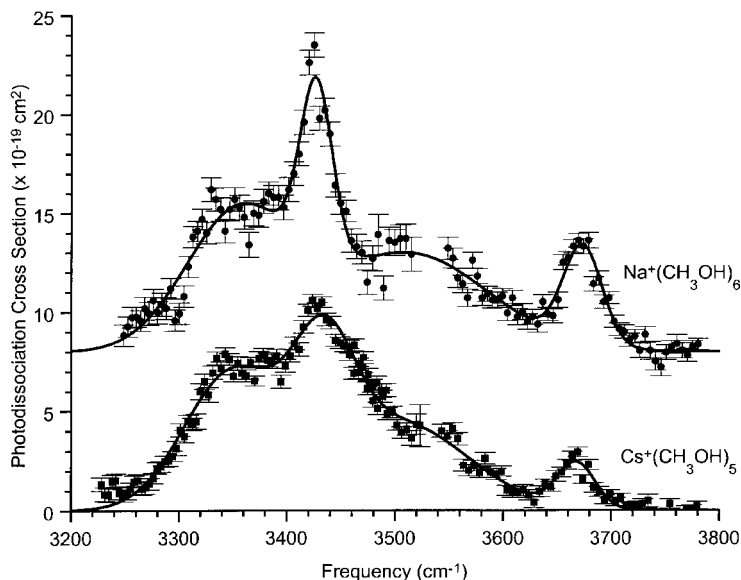


Figure 11. A comparison between the vibrational photodissociation spectra of  $\text{Cs}^+(\text{CH}_3\text{OH})_5$  and  $\text{Na}^+(\text{CH}_3\text{OH})_6$ . The error bars represent  $\pm 2\sigma$ . The curves are multiple Gaussian fits to the data. Note that the positions of the bands are very similar although there is some variation in the relative intensity.

question remains: can we characterize the solvent structure(s) associated with these hydrogen-bonded O—H vibrational frequencies? We can envisage that the answer must somehow be related to structures or configurations that occur in both cluster ions and that these structures are determined by methanol–methanol interactions. A logical deduction is that intrinsic methanol interactions are responsible and that an examination of neutral methanol clusters is in order.

The ability to make measurements on size-selected neutral clusters has been challenged by the difficulty in developing a universal method for size selection. In some cases, the ability to resolve vibrational features rotationally and to assign the spectra successfully has been extended beyond neutral trimers as is the case in water tetramer [53], pentamer [54] and hexamer [55] by Saykally and co-workers. Vibrational spectra have also been obtained using ion-dip spectroscopy by clustering molecules to a suitable aromatic host molecule that can be readily ionized by multiphoton ionization methods. Examples of this approach include the vibrational spectroscopy of  $\text{C}_6\text{H}_6-(\text{H}_2\text{O})_{1-6}$  by Pribble and Zwier [56] and  $\text{C}_6\text{H}_5\text{OH}-(\text{H}_2\text{O})_{1-6}$  by Mikami and co-workers [35–57] in the important O—H stretching region, where the extent and role of hydrogen bonding could be used to infer the cluster structures. More recently, Huisken *et al.* have applied the method of size selection via molecular beam scattering, developed by Muck and Meyer [58], to the vibrational spectroscopy of  $(\text{HF})_{4-8}$  [4],  $(\text{H}_2\text{O})_{2-5}$  [5] and  $(\text{CH}_3\text{OH})_3$  [6] in the 2.5–3.5  $\mu\text{m}$  region, to characterize the size dependence of hydrogen bonding. The importance of this work for methanol can be seen in table 1, where the vibrational frequencies observed in  $\text{Cs}^+(\text{CH}_3\text{OH})_{1-6}$  and  $\text{Na}^+(\text{CH}_3\text{OH})_{2-7}$  can be compared with vibrational frequencies for neutral methanol clusters. Although shifted by 15–50  $\text{cm}^{-1}$  to lower frequencies, the O—H vibrational frequencies in the ion clusters appear to correlate directly to specific neutral clusters. Since the vibrational features are independent of the ion, they must be intrinsically

Table 1. Vibrational frequencies of solvated metal ions and neutral methanol clusters. Uncertainties are in parentheses and linewidths are in italics.

	Vibrational frequency ( $\text{cm}^{-1}$ )				
	$\nu_{\text{monomer}}$	$\nu_{\text{dimer}}$	$\nu_{\text{trimer}}$	$\nu_{\text{tetramer}}$	$\nu_{\text{multimer}}$
Neutral methanol	3681 <sup>a</sup>	3574 <sup>b</sup>	3475 <sup>c</sup>	3378 <sup>d</sup>	3292 <sup>d</sup>
$\text{M}^+(\text{CH}_3\text{OH})_n$					
$\text{Cs}^+, n = 1$	3663(3) <i>108</i>				
$\text{Na}^+, n = 2$	3659(1) <i>110</i>				
$\text{Cs}^+, n = 2$	3665(1) <i>72</i>				
$\text{Na}^+, n = 3$	3667(1) <i>72</i>				
$\text{Cs}^+, n = 3$	3665(1) <i>54</i>		3414(4) <i>112</i>		
$\text{Na}^+, n = 4$	3670(1) <i>66</i>		3388(8) <i>85</i>		
$\text{Cs}^+, n = 4$	3668(3) <i>48</i>	3520(3) <i>124</i>	3415(2) <i>50</i>	3339(8) <i>86</i>	
$\text{Na}^+, n = 5$	3670(1) <i>46</i>	3519(1) <i>122</i>	3406(2) <i>54</i>		
$\text{Cs}^+, n = 5$	3667(1) <i>42</i>	3502(20) <i>153</i>	3434(3) <i>67</i>	3350(5) <i>106</i>	
$\text{Na}^+, n = 6$	3673(1) <i>42</i>	3515(1) <i>162</i>	3427(2) <i>34</i>	3357(7) <i>121</i>	
$\text{Cs}^+, n = 6$			3410(1) <i>221</i>		
$\text{Na}^+, n = 7$	3672(2) <i>41</i>	3511(15) <i>122</i>	3422(4) <i>81</i>	3341(4) <i>53</i>	3278(31) <i>69</i>

<sup>a</sup> From [52].

<sup>b</sup> From [54].

<sup>c</sup> From [6].

<sup>d</sup> From [59].

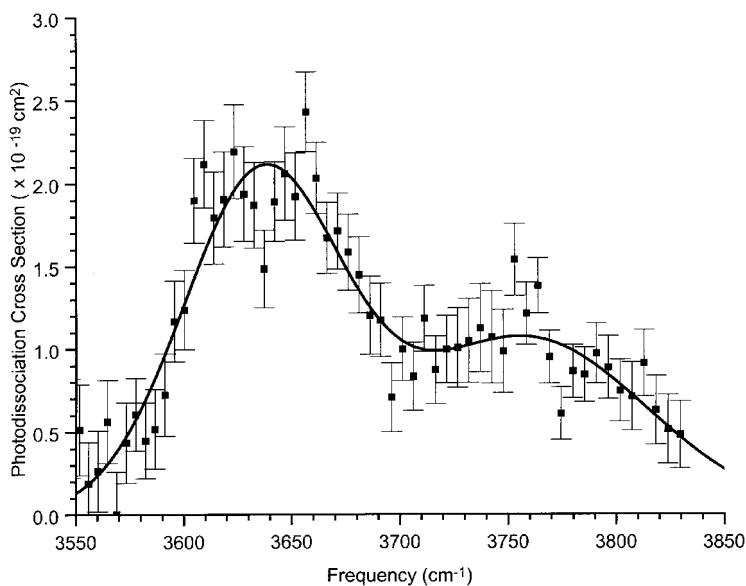


Figure 12. Vibrational photodissociation spectrum of  $\text{Cs}^+(\text{H}_2\text{O})$ . The error bars represent  $\pm 2\sigma$ . The curve is a double Gaussian fit to the data.

related to the properties of aggregates of methanol and, from table 1, these aggregates appear to be neutral methanol clusters of known size and structure. Thus, within the cluster ion, there appears to be specific methanol substructures, in forms such as methanol dimer, cyclic methanol trimer, tetramer and larger clusters, associated with the ion. They can be identified by their characteristic O—H stretching pattern. The presence of both cyclic trimer and tetramer bands in  $\text{Na}^+(\text{CH}_3\text{OH})_6$  requires the existence of structural isomers in the cluster ion beam, since both neutral clusters could not be attached to the same ion and still satisfy the mass-selected size requirement of six methanols. Inspection of the other infrared spectra with as few as three or four solvents also indicate that, once hydrogen bonding is observed in the system, structural isomers for a given cluster size are indeed the rule and not the exception. This is a very different situation from what is normally observed for cold neutral clusters in molecular beams, where structural isomers are a rarity.

The rich and informative infrared spectra of neutral clusters and solvated metal ions are not limited to methanol, as we shall now show with some initial spectra [41] of  $\text{Cs}^+(\text{H}_2\text{O})_{1-5}$ . The spectrum of  $\text{Cs}^+(\text{H}_2\text{O})_1$ , shown in figure 12, has an unusual feature of its own that is not possible in methanol. While the two apparent peaks due to the symmetric and asymmetric bands at 3636 and 3758  $\text{cm}^{-1}$  are only slightly shifted from the gas-phase values [60] of 3652 and 3756  $\text{cm}^{-1}$  respectively, there is a very distinct change in the intensities. In neutral water monomer, the intensity of the asymmetric O—H stretch is about 15 times greater than that for the symmetric stretch [61]. There are *ab initio* calculations on the vibrational properties of  $\text{Cs}^+(\text{H}_2\text{O})_1$ , as well as other hydrated alkali metal ions that suggest [38], while both vibrational intensities are enhanced, the intensity of the symmetric stretch has the greater gain, reducing the above ratio to slightly less than four. The relative intensities of the two O—H vibrations are the feature unique to water. The fit of the spectrum with two Gaussian functions yields nearly equal integrated cross-sections. The same *ab initio* calculations also predict shifts in the harmonic frequencies of  $-17$  and  $-39$   $\text{cm}^{-1}$  for the symmetric and asymmetric modes respectively, reflecting the small impact that the electrostatic interaction of the ion has on this particular vibrational attribute. These somewhat small shifts are qualitatively consistent with the experimental observations.

The vibrational spectra of larger hydrated caesium ions,  $\text{Cs}^+(\text{H}_2\text{O})_{3-4}$ , also contain the symmetric and asymmetric vibrations due to isolated water as shown in figure 13. The symmetric peak is unobscured at 3640  $\text{cm}^{-1}$ ; however, the asymmetric band is only observed as a shoulder to a new peak at about 3703  $\text{cm}^{-1}$ . Additional bands below 3600  $\text{cm}^{-1}$  first appear for  $\text{Cs}^+(\text{H}_2\text{O})_3$  and, like the peak at 3703  $\text{cm}^{-1}$ , also gain in intensity with increasing cluster size. These features, near 3470 and 3550  $\text{cm}^{-1}$ , are obviously due to hydrogen-bonded water that is associated with the caesium ion. Thus the onset for hydrogen bonding is observed for hydrated caesium ions at the same size as for caesium ions solvated by methanol. As in the case of methanol, the extent of hydrogen bonding increases with increasing size as reflected by the increase in the intensity for the hydrogen-bonded vibrational bands relative to the isolated water O—H stretching modes. However, it is important to note that the enhancement of the symmetric relative to the asymmetric stretch is maintained by isolated water molecules in the larger solvated ions. There is also the strong suggestion that structural isomers will be present in these hydrated ions as was the case in the metal ions solvated by methanol.

In a manner that was instructive for methanol, the sources for these new vibrational bands can be found from the experiments on size-selective neutral water



Table 2. Vibrational frequencies of hydrated caesium ions and neutral water clusters. Uncertainties from the fits are in parentheses.

	Vibrational frequency ( $\text{cm}^{-1}$ )					
	$\nu_{\text{sym}}$ monomer	$\nu_{\text{asym}}$ monomer	$\nu_{\text{free O—H}}$	$\nu_{\text{donor}}$ dimer	$\nu_{\text{cyclic}}$ trimer	$\nu_{\text{cyclic}}$ tetramer
Neutral water	3652 <sup>a</sup>	3756 <sup>a</sup>	3714 <sup>b</sup>	3601 <sup>b</sup>	3533 <sup>b</sup>	3416 <sup>b</sup>
$\text{Cs}^+(\text{H}_2\text{O})_n$						
$n = 1$	3636(3)	3758(20)				
$n = 2$	3636(2)	3758				
$n = 3$	3639(4)	3756	3701(2)	3540	3457(8)	
$n = 4$	3643(4)	3741(6)	3705(2)	3559(8)	3477(4)	
$n = 5$	3643(22)	NO <sup>c</sup>	3707(4)	NO <sup>c</sup>	3485(10)	3410(12)

<sup>a</sup> From [60].

<sup>b</sup> From [5].

<sup>c</sup> NO, Not observed.

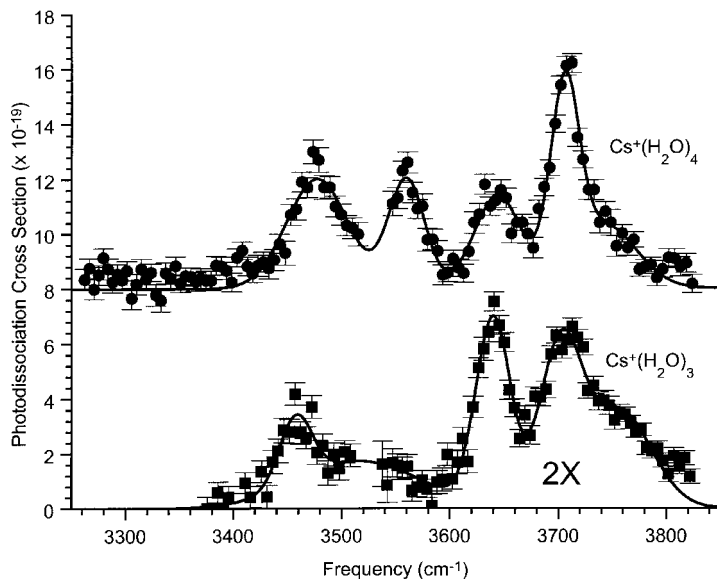


Figure 13. Vibrational photodissociation spectra of  $\text{Cs}^+(\text{H}_2\text{O})_{3,4}$ . The error bars represent  $\pm 2\sigma$ . The curves are multiple Gaussian fits to the data.

clusters from the laboratory of Huisken *et al.* [5]. These results are collected in table 2 for comparison with the results from the hydrated ion. The pattern of successive shifts to lower frequency with increasing size of neutral water clusters is reflected in the hydrogen-bonded bands of the hydrated caesium ion. In a manner similar to that for methanol, there is a one-to-one correspondence between the vibrational bands for the neutral water and hydrated ion. The isolated water and ‘free’ O—H stretch of a hydrogen-bonded water (the other O—H that is not participating as a proton donor in a hydrogen bond) are only slightly shifted ( $10\text{--}30\text{ cm}^{-1}$ ) to lower frequencies when complexed to ion. The hydrogen-bonded O—H stretches of the dimer, cyclic trimer and tetramer are generally shifted by larger amounts ( $10\text{--}70\text{ cm}^{-1}$ ) when complexed to

the caesium ion. This behaviour is essentially the same as was observed for the metal ions solvated by methanol. The presence of structural isomers in those hydrogen-bonded hydrated ions is also confirmed. It is also important to note that *ab initio* calculations on  $\text{Cs}^+(\text{H}_2\text{O})_3$  indicate a number of structural isomers within a few kilojoules per mole; the lowest appears to be the cyclic water trimer bound to the ion, although the choice of basis set and correlation level does affect the results [38]. Once again, we are able to identify specific solvent structures within the first solvent shell of the ion. The ramifications and potential applications of this effect will be discussed in the next section.

#### 4. Discussion

The vibrational spectroscopy of solvated metal ions has made considerable progress over the past few years. The ability to probe different vibrational modes in different spectral regions has been made possible by the application of a variety of infrared sources such as continuous-wave  $\text{CO}_2$  and pulsed  $\text{LiNbO}_3$  OPO lasers. This progress has been marked by the evolution of detail available in the description of the solvation process. At first, only the coarsest features were observed such as the size of the first solvent shell and the onset of bulk-like behaviour. With the advent of spectroscopy in the 3-0  $\mu\text{m}$  region, it is now possible to determine the configuration of the solvent molecules as the first solvent shell is filled. As was shown in the preceding section, there were a number of new and somewhat unexpected results associated with the solvation of caesium and sodium by methanol and water. Perhaps the most surprising was the early onset of hydrogen-bond formation. Monte Carlo simulations from our group and others [62] indicated that such interactions would first occur as the first shell was nearing completion for caesium and as the filling of the second shell commenced for sodium. However, we observed hydrogen bonds in much smaller solvated ions, with as few as three solvent molecules for caesium and four for sodium. It will be of great interest to examine other typical solvents that exhibit hydrogen bonding such as ammonia and ethanol, or molecules such as hydrogen fluoride and phenol. The degree to which molecules are able to hydrogen bond can thus be varied like other experimental variables such as size and charge density.

There were other notable results from these studies. The observation of structural isomers in the cluster ion beam at sizes that exhibited hydrogen bonding, will undoubtedly be of great interest to theoreticians. First, there is obvious evidence for a number of low-lying minima on the ground potential energy surface of these solvated ions. An accurate *ab initio* calculation, Monte Carlo or molecular dynamics simulation must be able to confirm the existence of the isomers. Second, by using information from neutral solvent cluster studies, the structure of these isomers has also been established, placing further demands on the accuracy of the theoretical results. The need for accurate and computationally efficient models of intermolecular interactions comes from the increasing use of molecular modelling methods for characterizing diverse problems such as protein folding [63] and drug design [64]. Finally, there was the surprising variation in the intensity of the symmetric and asymmetric O—H stretching frequencies, going from the water monomer to isolated waters complexed to the metal ion. The enhancement of the symmetric stretch was observed to be maintained for isolated water molecules in larger cluster ions where hydrogen-bonded water molecules were also present. This dramatic change in intensity appears to be due to the strong electrostatic effect that the ion has on the induced dipole moment of the symmetric stretch [65]. This transition moment lies along the symmetry axis of the molecule and the binding axis of the molecule to the ion. The transition moment of the

asymmetric stretch does not share this favourable orientation. This change in transition moment may prove to be a useful and universal indication of strong electrostatic interaction between a water molecule and an ion. As such, it may play an important role in characterizing the structural environment of a water molecule that exhibits no hydrogen bonding in a cluster ion.

It is now possible to evaluate the competition between various intermolecular forces at the microscopic level, such as electrostatic interactions as against hydrogen bonding, in ways that are sensitive to variations in charge density, size and solvent. The examination of the delicate balance of these interactions, present in solution, extends far beyond the solvation process alone. Some areas of further investigation will be offered as possible future extensions of size- and composition-selective spectroscopy.

An initial study of competitive solvation for the system  $\text{Cs}^+(\text{CH}_3\text{CO})_n(\text{CH}_3\text{OH})_m$  was undertaken using a continuous-wave  $\text{CO}_2$  laser and a single quadrupole mass spectrometer ion cluster apparatus [66]. A significant change in the C—O stretch was observed to take place between cluster ions of the composition ( $n = 3, m = 1$ ) and ( $n = 4, m = 1$ ). While this result was interpreted as the formation of a hydrogen bond between methanol and acetone, prior to the filling of the first solvent shell, it was somewhat unexpected. Monte Carlo simulations that accompanied the experimental study predicted the onset of hydrogen-bond formation at ( $n = 7, m = 1$ ) a much larger cluster although still before the filling of the first solvent shell. However, this is no longer a surprising result based on the detection of hydrogen bonding with as few as three methanols about the caesium ion as shown in the preceding section. This type of mixed-cluster study can now be undertaken with considerably more sensitivity to the environment of the methanol molecule. Indeed, the spectra of  $\text{Cs}^+(\text{CH}_3\text{CO})_n(\text{CH}_3\text{OH})_m$ , with  $m > 1$  in the C—O stretching region, were suggestive of different bonding environments for the methanols in these cluster ions, but a characterization of the structural variations could not be made. It should now be possible to look at these more complicated systems using the O—H stretching mode, which has been shown to be sensitive to intermolecular interactions with other molecules. It might well be possible to look at competitive solvation with two solvents capable of hydrogen bonding such as water and ammonia, where the O—H and N—H stretching modes are somewhat separated in frequency.

A separate aspect of the mixed solvent ion cluster may offer some insights into the dynamics and energetics of the dissipation of excess energy in finite systems. Mixed clusters of the type mentioned above,  $\text{Cs}^+(\text{CH}_3\text{CO})_n(\text{CH}_3\text{OH})_m$ , have two possible routes for evaporative loss. The comparative rate of the loss of methanol or acetone depends on the relative binding energies and the number of equivalent transition states for either channel. We have observed [50, 67] in  $\text{Na}^+(\text{CH}_3\text{CO})_n(\text{CH}_3\text{OH})_m$  a clear transition from loss of methanol to loss of acetone in clusters of composition with  $m = 1, 2, 3$  and  $n > 5 - m$ . In principle, these cluster ions are formed in the same evaporative ensemble and should be characterized by a common energy distribution. It will be extremely interesting to look at the correlation between dynamics (unimolecular dissociation rates and branching ratios) with structure (solvent shell occupation and hydrogen bonding).

The structural extensions of the mixed-ion-cluster methods may potentially be quite useful in the area of ion transport in biological systems. It is well known that biological systems have many ways of selecting ions by size for suitable transport. For size-selective protein ion channels, one mechanism involves an oxygen ‘bracelet’

formed from the amide carbonyls of the peptide backbone, where the physical size or diameter of the ring is the key factor [68]. An alternative mechanism, recently proposed, is based on the interaction between aromatic side-chains on the peptides and the cations [69]. Calculations on the 'cation- $\pi$ ' interaction involving clusters of benzene and the alkali metal ions [70] indicate the most stable complex with two benzenes and one alkali ion is with  $K^+$ . These same calculations also indicate that the binding energy for benzene to the alkali ions is comparable with the binding energy of water. Measurements on the enthalpies of association using HPMS by Kebarle and co-workers [71] for clusters of composition  $K^+(C_6H_6)_{1-3}(H_2O)_{1-3}$  are consistent with these results. There is the strong implication that interactions with aromatic side chains in the ion channel protein may be responsible for the preferential selection of  $K^+$  over  $Na^+$ . In a series of  $K^+$  gating channel proteins that have shown a strong preference for  $K^+$ , each protein has a Gly-Try-Gly sequence in the pore region and the channel is produced from a tetramer complex of proteins. The tyrosine side chains form a rectangular passage, which just fits the potassium ion [72]. In some preliminary evaporative dissociation and CID experiments on  $K^+(C_6H_6)_{1,2}(H_2O)_{1-3}$ , we have observed that the preferred dissociation channel is the loss of one water [73]. We plan to investigate further the O-H spectroscopy of this system to determine the binding locations of the water. We shall be able to distinguish whether the water interacts with the ion, and/or with other waters, based on our hydrated ion work [41], or whether the water interacts with benzene, by referring to the infrared studies of Pribble and Zwier [56] on neutral clusters of  $C_6H_6(H_2O)_{1-6}$ . By combining electrospray ionization methods with a triple quadrupole or similar apparatus, there is the exciting possibility of examining ion binding to small peptides in the presence of water, using infrared spectroscopy methods, to complement previous CID studies on ion-peptide interactions [74].

A second ion transport method involves the use of ionophores to transfer the ion across the cell membrane. Ionophores such as valinomycin and nonactin are known to bind potassium ions preferentially [75]. These systems have been frequently modelled in the past by chemically simpler systems such as the crown ethers. The size of the crown ether determines which alkali metal ions binds most effectively in solutions. However, it is important to note that the intrinsic binding of alkali metal ions to crown ethers [76] is always strongest for  $Li^+$ . The side-selective character of the crown ether in solution comes from the interaction between the ion and water. The delicate balance between ion-molecular and molecule-molecule interactions once again plays an important role. Infrared vibrational studies on size- and composition-selected clusters of an alkali ion, crown ethers and water molecules would permit this process to be examined at the microscopic level. It may indeed be possible to follow the transition from the intrinsic binding domain to the solution binding regime, by increasing the number of water molecules in the cluster ion. Then, perhaps with the use of electrospray technology, the binding of alkali ions with actual antibiotic ionophores in the presence of water could be studied spectroscopically.

## 5. Conclusions

The technical achievements in the vibrational spectroscopy of solvated metal ions can be attributed to a number of very favourable factors. The ability to mass-select cluster ions with the well established methods of mass spectrometry give us the capability to characterize both the size and the composition of a given species. The development and application of tunable infrared lasers in the  $3.0\ \mu\text{m}$  region to

these studies have permitted the direct investigation of hydrogen bonding in ions solvated by water and methanol. The concurrent successful studies of size-selective neutral clusters have assisted with the characterization of specific vibrational features that are associated with an individual neutral cluster. Finally, a one-to-one correspondence has been found between these vibrational bands in neutral and solvated ion clusters. Thus the vibrational spectroscopy of solvated metal ions has become much more than an examination of the solvation process. Structures within the first solvent shell of an ion can now be observed and characterized. These structures represent the competition between the electrostatic interaction of the ion with the solvent and the most important of intermolecular interactions: the hydrogen bond. Although these observations and interpretations rely on the collective information gained from different studies, this is no 'house of cards'. It is a solid foundation on which to examine the most basic tenets of physical chemistry: structure and dynamics.

The common theme for current and future investigations is the interplay between competing intermolecular interactions. The balance struck between these forces plays an important role in areas far beyond the domains of physical chemistry. As has already been discussed, there are logical extensions of this work from model systems such as  $K^+(C_6H_6)_{1,2}(H_2O)_{1-3}$ , to structural and binding questions of ions with peptides and ionophores, eventually leading to the mechanism of ion selectivity in channel proteins. This is just one potential area of investigation. The application and development of composition-selective techniques will continue to find their way from small molecule studies to physical and biophysical areas of importance. The excitement has just begun!

#### Acknowledgments

The author would like to express his thanks and gratitude to his present and former students who have worked with great enthusiasm and dedication over the past 8 years. They include Dr Wen-Long Liu, Dr Jeffrey A. Draves, Dr Thomas J. Selegue, Mr Neil Moe, Mr Ronald Smart, Mr Bryan Goodman and Mr Robert Lewis. The efforts of Mr Corey Weinheimer and Mr Orlando Cabarcos were instrumental in completing much of the recent work discussed in this paper. The author would also like to acknowledge respectfully the continued support of this research by the National Science Foundation through grant No. CHE-9111930 and grant No. CHE-9321175. The author would also like to thank Professor Tamotsu Kondow and his research group at the University of Tokyo for their hospitality, during the completion of this review, and to acknowledge the support of the Japan Society for the Promotion of Science, through a Fellowship that permitted travel to Japan.

#### References

- [1] CASTLEMAN, A. W., and KEESER, R. G., 1986, *Chem. Rev.*, **86**, 589; KEARLE, P., 1992, *J. Am. Soc. Mass Spectrom.*, **3**, 1; CASTLEMAN, A. W., and BOWEN, K. H., 1996, *J. phys. Chem.*, **100**, 12911.
- [2] DALLESKA, N. F., HONMA, K., and ARMENTROUT, P. B., 1993, *J. Am. chem. Soc.*, **115**, 12125; DALLESKA, N. F., TJELTA, B. L., and ARMENTROUT, P. B., 1994, *J. phys. Chem.*, **98**, 4191.
- [3] ANDERSON, S. G., BLADES, A. T., KLASSEN, J. S., and KEARLE, P. 1995, *Int. J. Mass Spectrom. Ion Proc.*, **141**, 217; KLASSEN, J. S., BLADES, A. T., and KEARLE, P., 1995, *J. chem. Phys.*, **99**, 15509.
- [4] HUISKEN, F., KALLOUDIS, M., KULCKE, A., LAUSH, C., and LISY, J. M., 1995, *J. chem. Phys.*, **103**, 5366.

- [5] HUISKEN, F., KALOUDIS, M., and KULCKE, A., 1996, *J. chem. Phys.*, **104**, 17.
- [6] HUISKEN, F., KALOUDIS, M., KOCH, M., and WERHAHN, O., 1996, *J. chem. Phys.*, **105**, 8965.
- [7] RAY, D., LEVINGER, N. L., PAPANIKOLAS, J. M., and LINEBERGER, W. C., 1989, *J. chem. Phys.*, **91**, 6533; ALEXANDER, M. L., LEVINGER, N. L., JOHNSON, M. A., RAY, D., and LINEBERGER, W. C., 1988, *J. chem. Phys.*, **88**, 6200; VORSA, V., CAMPAGNOLA, P. J., NANDI, S., LARSSON, M., and LINEBERGER, W. C., 1996, *J. chem. Phys.*, **105**, 2298.
- [8] BAILEY, C. G., KIM, J., and JOHNSON, M. A., 1996, *J. phys. chem.*, **100**, 16782; SERXNER, D., DESSENT, C. E. H., and JOHNSON, M. A., 1996, *J. chem. Phys.*, **105**, 7231; DESSENT, C. E. H., BAILEY, C. G., and JOHNSON, M. A., 1995, *J. chem. Phys.*, **103**, 2006, and references therein.
- [9] ARNOLD, S. T., HENDRICKS, J. H., and BOWEN, K. T., 1995, *J. chem. Phys.*, **102**, 39; SNODGRASS, J. T., COE, J. V., FRIEDHOFF, C. B., MCHUGH, K. M., ARNOLD, S. T., and BOWEN, K. H., 1995, *J. phys. Chem.*, **99**, 9675, and references therein.
- [10] MARKOVICH, M., GINIGER, R., LEVIN, M., and CHESHNOVSKY, O., 1991, *J. chem. Phys.*, **95**, 9416; 1991, *Z. Phys. D*, **20**, 69; MARKOVICH, M., POLLACK, S., GINIGER, R., and CHESHNOVSKY, O., 1994, *J. chem. Phys.*, **101**, 9344; 1993, *Z. Phys. D*, **26**, 98.
- [11] SHEN, M. H., and FARRAR, J. M., 1989, *J. phys. Chem.*, **93**, 4386; 1991, *J. chem. Phys.*, **94**, 3322.
- [12] DONNELLY, S. G., and FARRAR, J. M., 1993, *J. chem. Phys.*, **98**, 5450.
- [13] SANEKATA, M., MISAIZU, F., and FUKU, K., 1996, *J. chem. Phys.*, **104**, 9768.
- [14] MISAIZU, F., SANEKATA, M., TSUKAMOTO, K., FUKU, K., and IWATA, S., 1992, *J. phys. Chem.*, **96**, 8259; FUKU, K., MISAIZU, F., SANEKATA, M., TSUKAMOTO, K., and IWATA, S., 1993, *Z. Phys. D*, **26**, S180; MISAIZU, F., SANEKATA, M., FUKU, K., and IWATA, S., 1994, *J. chem. Phys.*, **100**, 1161.
- [15] SCURLOCK, C. T., PULLENS, S. H., and DUNCAN, M. A., 1996, *J. chem. Phys.*, **105**, 3579, and references therein.
- [16] LESSEN, D. E., ASHER, R. L., and BRUCAT, P. J., 1991, *J. chem. Phys.*, **95**, 1414; ASHER, R. L., BELLERT, T., BUTHELEZI, T., and BRUCAT, P. J., 1994, *chem. Phys. Lett.*, **277**, 623; ASHER, R. L., BELLERT, T., BUTHELEZI, T., WEERASEKERA, G., and BRUCAT, P. J., 1994, *Chem. Phys. Lett.*, **228**, 390.
- [17] SELEGUE, T. J., and LISY, J. M., 1992, *J. phys. Chem.*, **96**, 4143.
- [18] ICHIHASHI, M., YAMABE, J., MURAI, K., NONOSE, S., HIRAO, K., and KONDOW, T., 1996, *J. phys. Chem.*, **100**, 10050.
- [19] SELEGUE, T. J., MOE, N., DRAVES, J. A., and LISY, J. M., 1992, *J. chem. Phys.*, **96**, 7268.
- [20] DRAVES, J. A., LUTHEY-SCHULTEN, L., LIU, W.-L., and LISY, J. M., 1990, *J. chem. Phys.*, **93**, 4589.
- [21] WINKEL, J. F., WOODWARD, C. A., JONES, A. B., and STACE, A. J., 1995, *J. chem. Phys.*, **103**, 5177.
- [22] JONES, A. B., LOPEZ-MARTENS, R., and STACE, A. J., 1995, *J. phys. chem.*, **99**, 6333.
- [23] JONES, A. B., WOODWARD, C. A., WINKEL, J. F., and STACE, A. J., 1994, *Int. J. Mass Spectrom. Ion Proc.*, **133**, 83.
- [24] WINKEL, J. F., JONES, A. B., WOODWARD, C. A., KIRKWOOD, D. A., STACE, A. J., 1994, *J. chem. Phys.*, **101**, 9436.
- [25] NIZKORODOV, S. A., MAIER, J. P., and BIESKE, E. J., 1995, *J. chem. Phys.*, **102**, 5570; NIZKORODOV, S. A., DOPFER, O., RUCHTI, T., MEUWLY, M., MAIER, J. P., and BIESKE, E. J., 1995, *J. phys. Chem.*, **99**, 17118; BIESKE, E. J., NIZKORODOV, S. A., DOPFER, O., MAIER, J. P., STICKLAND, R. J., COTTRELL, B. J., and HOWARD, B. J., 1995, *Chem. Phys. Lett.*, **250**, 226; NIZKORODOV, S. A., MAIER, J. P., and BIESKE, E. J., 1995, *J. chem. Phys.*, **103**, 1297; MEUWLY, M., NIZKORODOV, S. A., MAIER, J. P., and BIESKE, E. J., 1996, *J. chem. Phys.*, **104**, 3876; NIZKORODOV, S. A., DOPFER, O., MEUWLY, M., MAIER, J. P., and BIESKE, E. J., 1996, *J. chem. Phys.*, **105**, 1770.
- [26] BIESKE, E. J., NIZKORODOV, S. A., BENNETT, F. R., and MAIER, J. P., 1995, *J. chem. Phys.*, **102**, 5152.
- [27] CHOI, J. H., KUWATA, K. T., CAO, Y., and OKUMURA, M., 1997 (to be published).
- [28] JOHNSON, M. S., KUWATA, K. T., WONG, C.-K., and OKUMURA, M., 1996, *chem. Phys. Lett.*, **260**, 551.
- [29] CHOI, J.-H., KUWATA, K. T., HASS, B.-M., CAO, Y., JOHNSON, M. S., and OKUMURA, M., 1994, *J. chem. Phys.*, **100**, 7153.
- [30] CAO, Y., CHOI, J.-H., HASS, B. M., and OKUMURA, M., 1994, *J. phys. Chem.*, **98**, 12176.

- [31] OKUMURA, M., YEH, L. I., and LEE, Y. T., 1988, *J. chem. Phys.*, **88**, 79.
- [32] YEH, L. I., OKUMURA, M., MYERS, J. D., PRICE, J. M., and LEE, Y. T., 1989, *J. chem. Phys.*, **91**, 7319.
- [33] PRICE, J. M., CROFTON, M. W., and LEE, Y. T., 1991, *J. phys. Chem.*, **95**, 2182.
- [34] BOO, D. W., and LEE, Y. T., 1995, *J. chem. Phys.*, **103**, 520.
- [35] MIKAMI, N., 1995, *Bull. chem. Soc. Japan*, **68**, 683.
- [36] SAWAMURA, T., FUJII, A., SATO, S., EBATA, T., and MIKAMI, N., 1996, *J. phys. Chem.*, **100**, 8131.
- [37] DRAVES, J. A., and LISY, J. M., 1990, *J. Am. chem. Soc.*, **112**, 9006; ZHANG, X., and CASTLEMAN, A. W., JR, 1992, *J. Am. chem. Soc.*, **114**, 9607; Selegue, T. J., and LISY, J. M., 1994, *J. Am. chem. Soc.*, **116**, 4874.
- [38] FELLER, D., GLENDENING, E. D., WOON, D. E., and FEYEREISEN, M. W., 1995, *J. chem. Phys.*, **103**, 3526; GLENDENING, E. D., and FELLER, D., 1995, *J. phys. Chem.*, **99**, 3060; and references therein.
- [39] BERNARDO, D. N., DING, Y., KROGH-JESPERSEN, K., and LEVY, R. M., 1994, *J. phys. Chem.*, **98**, 4180; Rick, S. W., Stuart, S. J., and BERNE, B. J., 1994, *J. chem. Phys.*, **101**, 6141; DANG, L. X., 1992, *J. chem. Phys.*, **96**, 6970; 1992, *ibid.*, **97**, 2659; KAMINSKI, G., and JORGENSEN, W. L., 1996., *J. phys. Chem.*, **100**, 18010.
- [40] SEARCY, J. Q., and FENN, J. B., 1974, *J. chem. Phys.*, **61**, 5282.
- [41] WEINHEIMER, C. J., and LISY, J. M., 1996, *J. chem. Phys.*, **105**, 2938.
- [42] WEINHEIMER, C. J., and LISY, J. M., 1996, *J. phys. Chem.*, **100**, 15305.
- [43] WEINHEIMER, C. J., and LISY, J. M., 19096, *Int. J. Mass. Spectrom. Ion Proc.* (to be published).
- [44] HUISKEN, F., and STEMMLER, M., 1988, *Chem. Phys. Lett.*, **146**, 391; LACOSSE, J. P., and LISY, J. M., 1990, *J. phys. Chem.*, **94**, 4398; Buck, U., Schmidt, B., and SIEBERS, J. G., 1993, *J. chem. Phys.*, **99**, 9428; BUCK, U., and ETTISCHER, I., 1994, *J. chem. Phys.*, **100**, 6974. BUCK, U., 1994, *J. phys. Chem.*, **98**, 5190.
- [45] FRASER, G. T., NELSON, D. D., JR, CHARO, A., and KLEMPERER, W., 1985, *J. Chem. Phys.*, **82**, 2353; Snels, M., Fantoni, R., Sanders, R., and MEERTS, W. L., 1987, *chem. Phys.*, **115**, 79; Heijman, B., Bizzari, A., Stolte, S., and REUSS, J., 1988, *chem. Phys.*, **126**, 201; Huisken, F., and PERTSCH, T., 1988, *Chem. Phys.*, **126**, 213.
- [46] AULT, B. S., 1978, *J. Am. chem. Soc.*, **100**, 5773.
- [47] BUCK, U., GU, X., HOBEIN, M., KROHNE, R., LAVENSTEIN, C., LINNARTZ, H., and RUDOLPH, A., 1991, *Z. Phys, D*, **20**, 177.
- [48] SELEGUE, T. J., MOE, N., and LISY, J. M., 1993, *Z. Phys, D*, **26**, 207.
- [49] NEHER, E., 1992, *Science*, **256**, 498; SACKMANN, B., 1992, *Science*, **256**, 503.
- [50] LISY, J. M., 1996, *Structure and Dynamics of Clusters*, edited by T. KONDOW, K. KAYA and A. TERASAKI (Tokyo: University Academy Press), p. 95.
- [51] KLOTS, C. E., 1987, *Z. Phys. D*, **5**, 83.
- [52] SHIMANOUCI, T., 1972, *Tables of Molecular Vibrational Frequencies*, Vol. 1 National Standards Reference Data series.
- [53] CRUZAN, J. D., BRALY, L. B., LIU, K., BROWN, M. G., LOESER, J. G., and SAYKALLY, R. J., 1996, *Science*, **271**, 59.
- [54] LIU, K., BROWN, M. G., CRUZAN, J. D., and SAYKALLY, R. J., 1996, *Science*, **271**, 62.
- [55] LIU, K., BROWN, M. G., CARTER, C., SAYKALLY, R. J., GREGORY, J. K., and CLARY, D. C., 1996, *Nature*, **381**, 501.
- [56] PRIBBLE, R. N., and ZWIER, T. S., 1994, *Science*, **265**, 75.
- [57] TANABE, S., EBATA, T., FUJII, M., and MIKAMI, N. 1993, *chem. Phys. Lett*, **215**, 347.
- [58] BUCK, U., and MEYER, H., 1984, *Phys. Rev. Lett.*, **52**, 109.
- [59] LUCK, W. A. P., and SCHREMS, O., 1980, *J. Molec. Struct.*, **60**, 333.
- [60] HERZBERG, G., 1945, *Infrared and Raman Spectra* (New York: Litton Educational Publishing), p. 281.
- [61] ROTHMAN, L. S., GAMACHE, R. R., TIPPING, R. H., RINSLAND, C. P., SMITH, M. A. H., BENNER, C. D., MALATHY DEVI, V., FLAUD, J.-M., CAMY-PEYRET, C., PERRIN, A., GOLDMAN, A., MASSIE, S. T., BROWN, L. R., and TOTH, R. A., 1992, *J. quant. Spectrosc. radiat. Transfer*, **48**, 469.
- [62] JORGENSEN, W. L., BIGOT, B., and CHANDRASEKHAR, J., 1982, *J. Am. chem. Soc.* **104**, 4584; CHANDRASEKHAR, J., and JORGENSEN, W. L., 1982, *J. chem. Phys.*, **77**, 5080.

- [63] DOYE, J. P. K., and WALES, D. J., 1996, *J. chem. Phys.*, **105**, 8428.
- [64] SCAPOZZA, L., ROGNAN, D., FOLKERS, G., and DASER, A., 1995, *Acta Crystallogr. D*, **51**, 541.
- [65] IWATA, S., 1996, private communication.
- [66] SELEGUE, T. J., CABARCOS, O. C., and LISY, J. M., 1994, *J. Chem. Phys.*, **100**, 4790.
- [67] WEINHEIMER, C., and LISY, J. M., 1997, unpublished work.
- [68] HILLE, B., 1991, *Ionic Channels of Excitable Membranes* second edition (Sunderland, Massachusetts: Sinauer).
- [69] HEGINBOTHAM, L., and MACKINNON, R., 1992, *Neuron*, **8**, 483; Dougherty, D. A., 1996, *Science*, **271**, 163.
- [70] DOUGHERTY, D., 1993, *Science*, **261**, 1708.
- [71] SUNNER, J., NISHIZAWA, K., and KEBARLE, P., 1981, *J. phys. Chem.*, **85**, 1814.
- [72] DURELL, S. R., and GUY, H. R., 1992, *Biophys. J.*, **62**, 238.
- [73] WEINHEIMER, C., and LISY, J. M., 1997, unpublished results.
- [74] ZHAO, H., REITER, A., TEESCH, L. M., and ADAMS, J., 1993, *J. Am. chem. Soc.*, **115**, 2854, and references therein; HU, P., and GROSS, M. L., 1992, *J. Am. chem. Soc.*, **114**, 9153, and references therein.
- [75] DOBLER, M., 1981, *Ionophores and Their Structures* (New York: Wiley).
- [76] CHU, I.-H., ZHANG, H., and DEARDEN, D. V., 1993, *J. Am. chem. Soc.*, **115**, 5736.